

# Complete parameter identification of parallel manipulators with partial pose information using a new measurement device

## Abdul Rauf\*, Sung-Gaun Kim and Jeha Ryu

\*Department of Mechatronics, Kwangju Institute of Science and Technology, 1 Oryong-dong, Buk-Gu, Gwangju 500-712 (Republic of Korea)  
E-mail: ryu@kjist.ac.kr

(Received in Final Form: January 19, 2004)

### SUMMARY

A new measurement device is proposed for the calibration of parallel manipulators that can be used to identify all kinematic parameters with partial pose measurements. The device while restricting the motion of the end-effector to five degree-of-freedom measures three components of posture. A study is performed for a six degree-of-freedom fully parallel Hexa Slide Manipulator. Intrinsic inaccuracies of the measurement device are modeled with two additional identification parameters. Computer simulations show that all parameters, including the additional parameters, can be identified. Results show a significant error reduction, even with noisy measurements, and reveal that the identification is robust against errors in initial guess.

**KEYWORDS:** HexaSlide manipulator; Identification parameters; Kinematic calibration; Measurement devices; Parallel robots

### 1. INTRODUCTION

Parallel manipulators are preferred to serial manipulators for their better dynamic capabilities, increased rigidity and high positioning accuracy. The latter, however, may deteriorate by factors like manufacturing tolerances, installation errors and link offsets resulting in different kinematic parameters from those of the nominal model. Kinematic calibration is a process by which the actual kinematic parameters are estimated and later used by the manipulator's controller. This compensates for the above sources of geometric errors and hence improves accuracy significantly. Without calibration, the significance and veridicality of results for experimental robotics cannot be gauged. One may expect to spend most of experimental effort in calibration and less in actually running the experiments in control.<sup>1</sup>

Kinematic calibration requires redundant sensory information. This information can be acquired by using external sensors,<sup>2–7</sup> or by adding extra sensors to the system,<sup>8–10</sup> or by restraining the motion of the end-effector through some locking device.<sup>11–17</sup> The latter two are categorized as self-calibration schemes.

Classical methods of calibration require measurement of complete or partial postures using some external measurement devices. Numerous devices have been used

for calibration of parallel manipulators. Zhuang et al.<sup>2</sup> used electronic theodolites for the calibration of the Stewart platform along with standard measurement tapes. For a 3 degree-of-freedom (DOF) redundant parallel robot, Nahvi et al.<sup>3</sup> employed LVDT sensors. Laser displacement sensors were used to calibrate a delta-4 type parallel robot by Maurine.<sup>4</sup> Ota et al.<sup>5</sup> performed calibration of a parallel machine tool, HexaM, using a Double Ball Bar system. Takeda et al.<sup>6</sup> proposed the use of a low order Fourier series to calibrate parallel manipulators involving the Double Ball Bar system. Besnard et al.<sup>7</sup> demonstrated that the Gough-Stewart platform could be calibrated using two inclinometers. All of the kinematic parameters can be identified when the Cartesian posture is completely measured. However, measuring all components of the Cartesian posture, particularly the orientation, can be difficult and expensive. With partial pose measurements, the experimental procedure is simpler but some of the parameters may not be identified. This may result in a significant variation of accuracy within the workspace.

Self-calibration schemes provide economic, automatic, non-invasive and fast data measurement and are therefore preferred over classical calibration methods. Zhuang<sup>8,9</sup> proposed two rotary sensors at each universal joint of alternate legs of the Stewart platform and discussed the formulation of a measurement residual and identification Jacobian in detail. Wampler et al. calibrated the Gough-Stewart platform using 5 sensors at passive joints of one leg.<sup>10</sup> Khalil and Besnard<sup>11</sup> showed that locking universal and/or spherical joints, with appropriate locking mechanisms, could calibrate the Stewart mechanism autonomously. Maurine et al.<sup>12–14</sup> extended the idea to calibrate HEXA-type parallel robot. Meggiolaro et al.<sup>15</sup> presented a calibration method using a single end-point contact constraint for a serial manipulator that has elastic effects due to end-point forces and moments. Rauf and Ryu,<sup>16</sup> and Ryu and Rauf<sup>17</sup> proposed calibration procedures for parallel manipulators by imposing constraints on the end-effector. The problem of non-identifiable parameters becomes severe for the self-calibration schemes, particularly for the fully autonomous calibration schemes that rely on imposing constraints.

Zhuang et al.<sup>12</sup> formulated the cost function in terms of the inverse kinematic residuals that results in a block diagonal identification Jacobian matrix, and the identification

procedure can be implemented without solving forward kinematics. Fassi et al.<sup>18</sup> proposed a procedure for obtaining a minimum, complete, and parametrically continuous model for the geometrical calibration of parallel robots. Iurascu and Park<sup>19</sup> formulated the kinematic calibration problem for closed chain mechanisms in a coordinate-invariant fashion and solved directly the nonlinear constrained optimization problem of calibration. Daney et al.<sup>20</sup> presented variable elimination technique to improve the effectiveness of identification procedure when only partial pose information is available. Khalil et al.<sup>21</sup> presented an algorithm to calculate the identifiable parameters for robots with tree structures. Oilivers et al.<sup>22</sup> used singular value decomposition for the identification process and showed that this provides immunity to numerical redundancies that may result from partial pose measurements. Based on QR analyses of the identification Jacobian matrix, Besnard and Khalil<sup>23</sup> analyzed numerical relations between the identifiable and the non-identifiable parameters for different calibration schemes with a case study on the Gough-Stewart platform that has 42 identification parameters. They showed that 3 parameters couldn't be identified when only position is measured, 7 parameters are non-identifiable when two inclinometers are used, and the maximum number of identifiable parameters with self-calibration schemes realized by imposing constraints is 30.

The partial pose measurement schemes studied so far considered only position or only orientation components and, therefore, cannot identify all parameters. Measuring component(s) of position and orientation simultaneously may identify all parameters. This paper presents a new measurement device for calibration of parallel manipulators that can measure two components of position along with a rotation. Note that the position components are measured in terms of angle and thus the cost function and the Identification Jacobian are homogenous. A study is performed for a 6-DOF fully parallel Hexa Slide manipulator. The device, however, is general and can be employed for other parallel manipulators. Two additional identification parameters are defined to model intrinsic inaccuracies of the device. Computer simulations show that all parameters can be identified with the measurements from the proposed device. QR analysis verifies the results of simulations. Measurement of postures can be automated, thereby making the experimental procedure simple.

This paper is organized as follows: Hexa Slide Manipulator (HSM) and its kinematics are described in Section 2. Section 3 discusses the calibration device along with measurement procedure and formulation. Results of computer simulations are presented in section 4. Section 5 concludes the study.

## 2. KINEMATICS OF THE MECHANISM

This section introduces the parallel robot, HSM, to which the proposed calibration scheme is applied and presents its kinematics. The schematic of the HSM is shown in figure 1 and the geometric parameters are defined in figure 2. It is a 6 DOF fully parallel manipulator of the PRRS type. In figure 2,  $A_{i0}$  and  $A_{i1}$  denote the start and the end points of the  $i$ th ( $i = 1, 2, \dots, 6$ ) rail axis.  $A_i$  denotes the center of  $i$ th universal

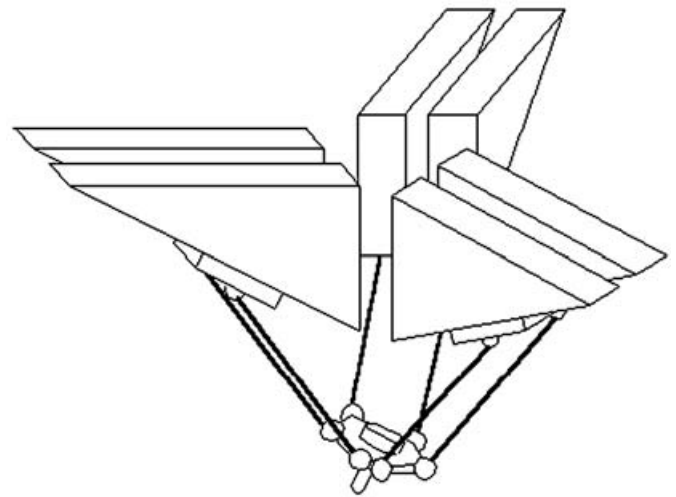


Fig. 1. Schematic of the HSM.

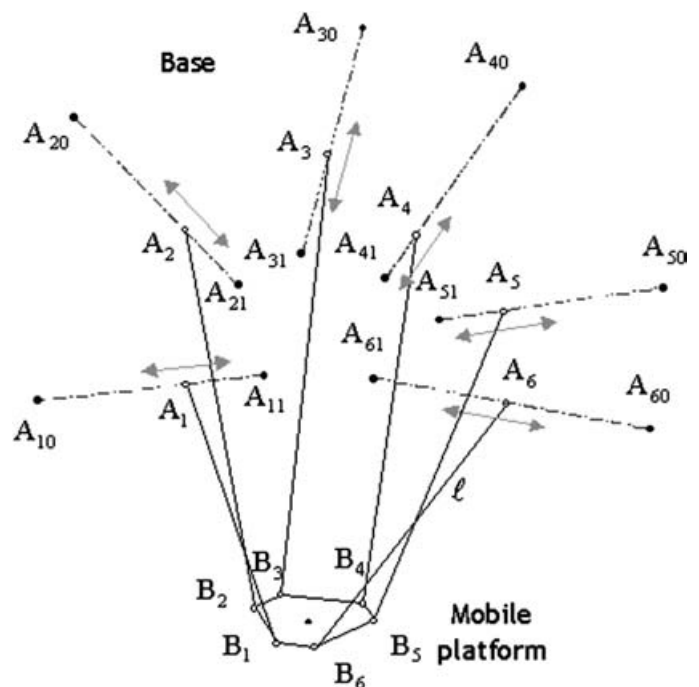


Fig. 2. Geometric parameters of the HSM.

joint and it lies on the line segment  $A_{i0}A_{i1}$ . Rail axes are identical and the nominal link length,  $\ell$ , is equal for all kinematic chains. The articular variable,  $\lambda_i$ , is the distance between the points  $A_{i0}$  and  $A_i$ .  $B_i$  denotes the center of  $i$ th spherical joint at the mobile platform.

The posture of the mobile platform is presented by the position of the mobile frame center in the base frame and three Euler angles as

$$\mathbf{X} = [x \quad y \quad z \quad \psi \quad \theta \quad \phi] \quad (1)$$

The Euler angles are defined as:  $\psi$  rotation about the global X-axis,  $\theta$  rotation about the global Y-axis and  $\phi$  rotation about the rotated local z-axis. Orientation is thus given by

$$\mathbf{R} = \mathbf{R}_{Y,\theta} \mathbf{R}_{X,\psi} \mathbf{R}_{Z,\phi}$$

$$\mathbf{R} = \begin{bmatrix} C\theta C\phi + S\theta S\phi S\psi & -C\theta S\phi + S\theta S\psi C\phi & S\theta C\psi \\ C\psi S\phi & C\psi C\phi & -S\psi \\ -S\theta C\phi + C\theta S\psi S\phi & S\theta S\phi + C\theta S\psi C\phi & C\theta C\psi \end{bmatrix} \quad (2)$$

where  $C$  and  $S$  represent the cosine and sine, respectively.

The problem of inverse kinematics is to compute the articular variables for a given position and orientation of the mobile platform. For the HSM, the problem of inverse kinematics is simple and unique and is solved individually for each kinematic chain. Considering a single link chain, the inverse kinematics relation can be expressed as

$$\lambda = \mathbf{a}^T \mathbf{A}_0 \mathbf{B} - \sqrt{\ell^2 - \|\mathbf{A}_0 \mathbf{B}\|^2 + (\mathbf{a}^T \mathbf{A}_0 \mathbf{B})^2} \quad (3)$$

where  $\mathbf{a}$  represents the direction vector of the slider.

In forward kinematics, posture (position and orientation) of the mobile platform is computed for given values of articular variables. Forward kinematics may yield multiple solutions and is solved numerically using an iterative procedure.<sup>24</sup>

$$\mathbf{X}_{k+1} = \mathbf{X}_k + \mathbf{J}_f(\lambda - \lambda_k) \quad (4)$$

where  $\mathbf{J}_f$  is the inverse Jacobian of Euler angles.

### 3. CALIBRATION DEVICE AND PROCEDURE

#### 3.1. The measurement device

A measurement device is proposed to measure simultaneously components of the position and orientation of the end-effector. The proposed device consists of a link having U joint at both ends. At one end, after the U joint, a rotary sensor is attached such that its axis of rotation passes through the U joint center. At the other end, a flange is provided for mounting. The device is also equipped with a biaxial inclinometer that measures rotations about X and Y-axes. Inclinometers are inertial devices and provide measurements with respect to “true vertical” – the direction of gravity. Biaxial inclinometers provide measurements about two mutually perpendicular axes. Figure 3 shows the labeled schematics of the proposed device.

The device provides position information of the end-effector in terms of the angles measured by the inclinometers. Note that although all three components can be computed for given angles, only two are independent. Rotary sensor directly measures rotation of the end-effector about the local z-axis when it is attached to the end-effector. Alternately, it can be coupled to the base and measure the rotation about the global Z-axis. Note that it is better to define orientation of the end-effector in terms of the measured angle or a transformation would be required.

#### 3.2. Frames and identification parameters

The origin of the base frame,  $O$ , is located at the center of the U joint near the base plate. The global Z-axis is directed

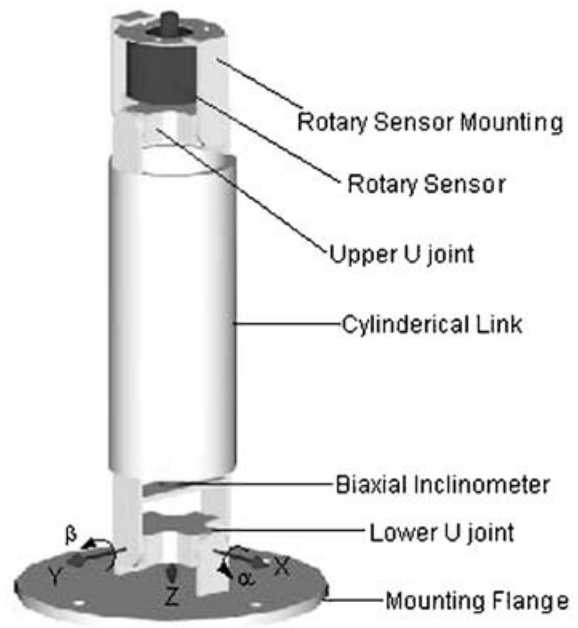


Fig. 3. Schematic of the proposed measurement device.

along the negative direction of the gravity acceleration and the global X-axis is defined parallel to the first measurement axis of the biaxial inclinometer. OXYZ system forms a right-handed system. The origin of the mobile frame,  $P$ , is located at the center of the U joint with Z-axis being collinear with the rotation axis of the rotary sensor. PX'Y'Z' also forms a right-handed system.

The number of identification parameters depends on the way the reference frames are assigned. By assigning the reference frames properly, the complexity of the calibration problem can be significantly reduced. Fassi et al.<sup>18</sup> discussed the manipulator under consideration for their study and concluded that the minimum, complete and parametrically continuous model for geometrical calibration can be described by 54 parameters, which is the same as considered in this study. The minimum and independent identification parameters for a kinematic chain of the HSM are as follows:

- S joints' location ( $\mathbf{B}$ ) – 3 parameters/chain
- Slider axis start point ( $\mathbf{A}_0$ ) – 3 parameters/chain
- Slider's direction vector ( $\mathbf{a}$ ) – 2 parameters/chain
- Link length ( $\ell$ ) – 1 parameter/chain

Note that the direction vectors of the sliders' are specified by two components; say  $x$  and  $y$ . This makes 9 parameters for each kinematic chain and a total of 54 parameters. Note also that all parameters are measured in the units of length.

In addition to the parameters of the HSM, the following two identification parameters are defined to model the inaccuracies of the proposed measurement device

- Angle between the measurement axes of the biaxial inclinometer –  $\gamma$
- Length of the proposed Link –  $L$

3.3. Measurement data

Mobile platform can only execute 5 DOF motions while the device is attached. It can then be positioned over a spherical surface with arbitrary orientation. For each posture, the rotation of the rotary sensor and two angles of the biaxial inclinometer are measured. If  $L$  is the length of the device, the distance between the U joint centers, and  $\alpha$  and  $\beta$  are the measured rotations about X and Y-axes, then position of the end-effector can be obtained as

$$\begin{aligned} x &= -L \cos(\alpha) \sin(\beta) \\ y &= L \sin(\alpha) \\ z &= -L \cos(\alpha) \cos(\beta) \end{aligned} \tag{5}$$

For values of  $x, y,$  and  $z,$  computed from forward kinematics for given articular variables, angles  $\alpha$  and  $\beta$  can be computed as

$$\begin{aligned} \alpha &= \sin^{-1}(y/L) \\ \beta &= \tan^{-1}(x/z) \end{aligned} \tag{6}$$

Note that the forward kinematics may converge to other than the desired solution. Therefore, each measurement needs to be checked, say by its Euclidian distance to the nominal posture, before using it for the calibration. Note also that position of the end-effector is represented in terms of angles in (6), which results in a homogenous cost function and identification Jacobian.

Equation (6) provides computed values of  $\alpha$  and  $\beta$  when the two measurement axes are exactly perpendicular. If  $\gamma$  is the actual angle between the measuring axes of the inclinometer (nominal value =  $\pi/2$ ), the system of equations presented in (6) can be rewritten as

$$\begin{aligned} x &= -L S \gamma ((C \beta - 1) C \gamma S \alpha + C \alpha S \beta) \\ y &= L (C \gamma C \alpha S \beta + S \alpha (C^2 \gamma C \beta + S^2 \gamma)) \\ z &= -L (C \alpha C \beta - C \gamma S \alpha S \beta) \end{aligned} \tag{7}$$

Equation (7) is solved numerically with initial guess from (6) to compute  $\alpha$  and  $\beta$ .

3.4. The identification loop

Typically, solving the following system of equations with least squares performs the identification for the calibration schemes

$$d\mathbf{u} = \mathbf{J}^{-1} d\mathbf{X} \tag{8}$$

where  $\mathbf{J}$  is the identification Jacobian,  $d\mathbf{X}$  is the vector of error residuals, i.e. the cost function to be minimized, and  $d\mathbf{u}$  is the vector to update the nominal parameters. The termination criterion is specified either on  $d\mathbf{u}$  or  $d\mathbf{X}$ , to solve (8) iteratively. Figure 4 shows the typical flow chart to implement (8), where  $\mathbf{V}^m$  is the vector of articular variables,  $\mathbf{X}^m$  is the vector of measured variables, and  $\mathbf{X}^k$  is the vector of computed variables at kth iteration.

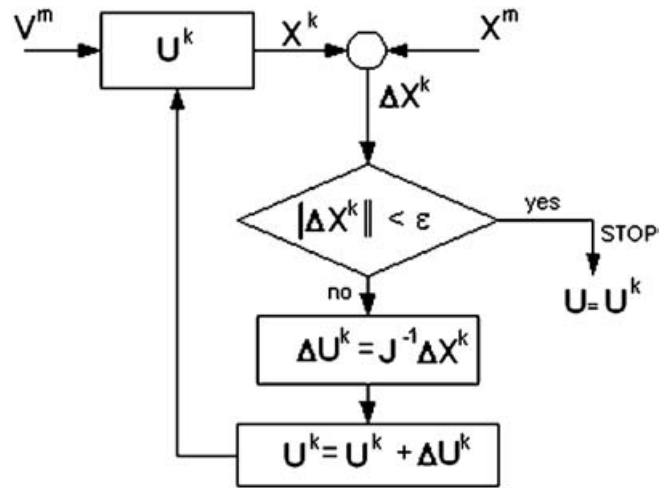


Fig. 4. Typical identification loop.

Three rows of the cost function and the identification Jacobian are computed for each measurement as

$$\begin{bmatrix} X_{i1} \\ X_{i2} \\ X_{i3} \end{bmatrix} = \begin{bmatrix} \alpha_m^i - \alpha_c^i \\ \beta_m^i - \beta_c^i \\ \phi_m^i - \phi_c^i \end{bmatrix} \tag{9}$$

$$\begin{bmatrix} J_{i1} \\ J_{i2} \\ J_{i3} \end{bmatrix} = \begin{bmatrix} \frac{\partial \alpha^i}{\partial u^1} & \frac{\partial \alpha^i}{\partial u^2} & \dots & \frac{\partial \alpha^i}{\partial u^{55}} \\ \frac{\partial \beta^i}{\partial u^1} & \frac{\partial \beta^i}{\partial u^2} & \dots & \frac{\partial \beta^i}{\partial u^{55}} \\ \frac{\partial \phi^i}{\partial u^1} & \frac{\partial \phi^i}{\partial u^2} & \dots & \frac{\partial \phi^i}{\partial u^{55}} \end{bmatrix} \tag{10}$$

where the subscripts  $m$  and  $c$  correspond, respectively, to the measured and the computed values. Note that the Identification Jacobian is computed for 55 parameters. The length of the measurement device,  $L$ , should also be treated as an identification parameter because of its fabrication tolerance. However, when added to the Identification Jacobian, it makes the matrix rank deficient. QR analyses also reveal that  $L$  cannot be treated as an independent parameter. Therefore,  $L$  is treated as a dependant identification parameter and is computed separately. The fact that the distance of the end-effector from origin of the base frame remains the same for each measured posture is exploited to compute the updated value of  $L$ . Postures are computed with updated identification parameters and then  $L$  is updated by minimizing the error in computed lengths. The loop of figure 4 is modified to update  $L$  at later stage as shown in figure 5. The nonlinear optimization function, "lsqnonlin", of the MATLAB optimization toolbox is used to find the updated value of  $L$ .

4. SIMULATIONS AND RESULTS

To study the validity and effectiveness of the proposed calibration device and procedure, computer simulations have been performed. For simulations, four sets of geometrical parameters are used. The first set defines the exact geometric parameters and is used to generate the measurement data.



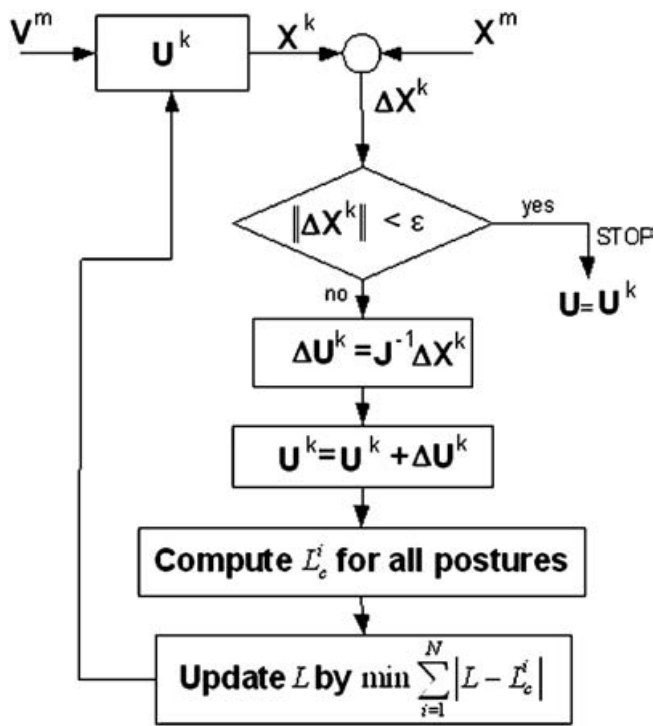


Fig. 5. Modified identification loop.

The other sets are used as nominal geometric parameters that should be calibrated. Table I gives the exact values of the geometric parameters and Table II shows the errors in the

Table I. The Exact geometric parameters.

#	1	2	3	4	5	6
$\mathbf{A}_{ox}$	-735.9	-841.8	-110.1	110.2	839.7	729.7
$\mathbf{A}_{oy}$	-552.2	-358.9	899.1	897.2	-355.6	-546.3
$\mathbf{A}_{oz}$	261.4	259.9	253.4	251.8	256.3	253.9
$\mathbf{B}_x$	-61.1	-170.8	-110.2	109.8	173.8	63.7
$\mathbf{B}_y$	-161.7	28.8	137.1	137.2	28.8	-161.7
$\mathbf{B}_z$	-16.1	-16.2	-16.1	-15.8	-16.1	-016.2
$\ell$	994.7	994.8	994.6	994.7	994.8	994.7
$\mathbf{a}_x$	750.2	749.8	0.2	-0.2	-749.7	-750.3
$\mathbf{a}_y$	433.2	432.7	-866.2	-866.3	432.9	432.7

Table II. Errors in the nominal parameters.

Parameters	Maximum	Mean	$\sigma$
Nominal Set 1	1.8	0.8	0.87
Nominal Set 2	2.8	1.33	1.45
Nominal Set 3	9.2	4.99	5.28

nominal sets used. Note that all dimensions in Table I and Table II are linear and are measured in millimeters. Exact values for the  $L$  and  $\gamma$  used are 750 mm and  $90^\circ$ . Nominal values of  $L$  used for three nominal sets are 749.3, 750.8, and 748.7 mm respectively and the nominal values of  $\gamma$  used are  $89.5^\circ$ ,  $90.7^\circ$ , and  $89^\circ$ .

Postures were generated with ranges along X and Y-axes, being  $\pm 350$  millimeters from the origin. The range for

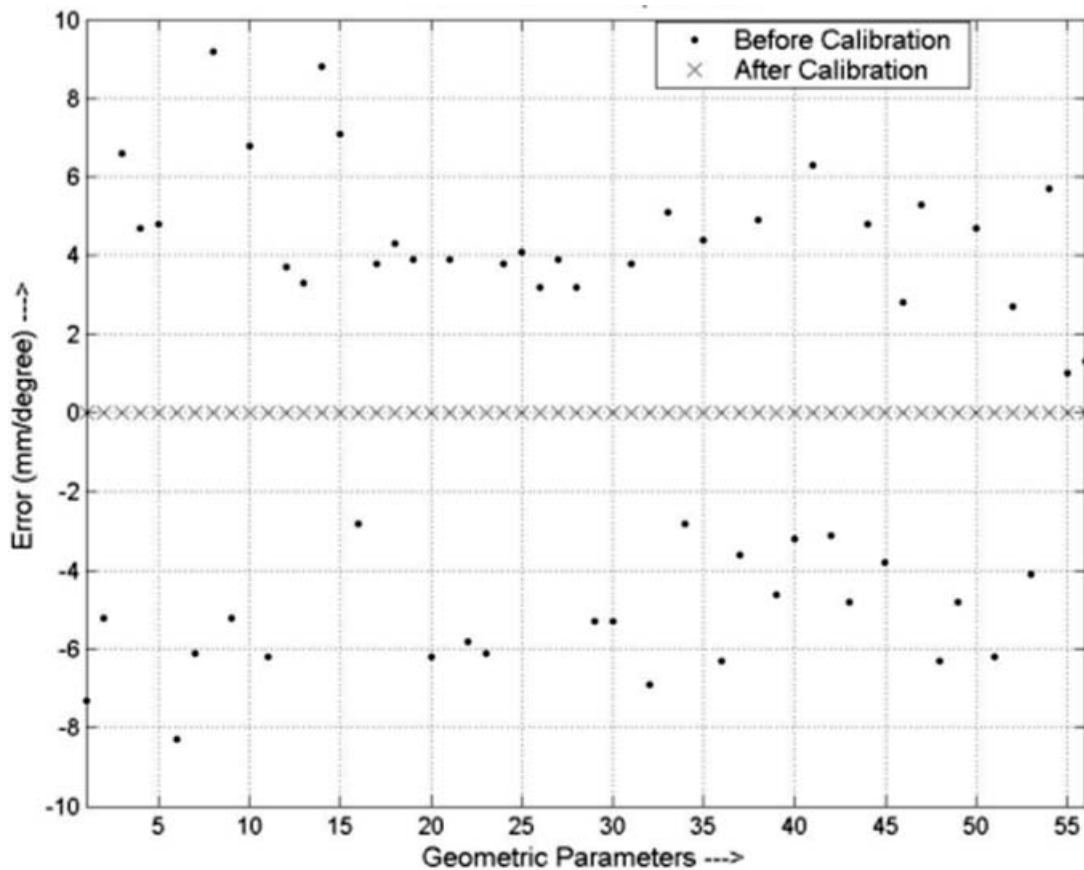


Fig. 6. Identification without noise (Nominal Set 3).

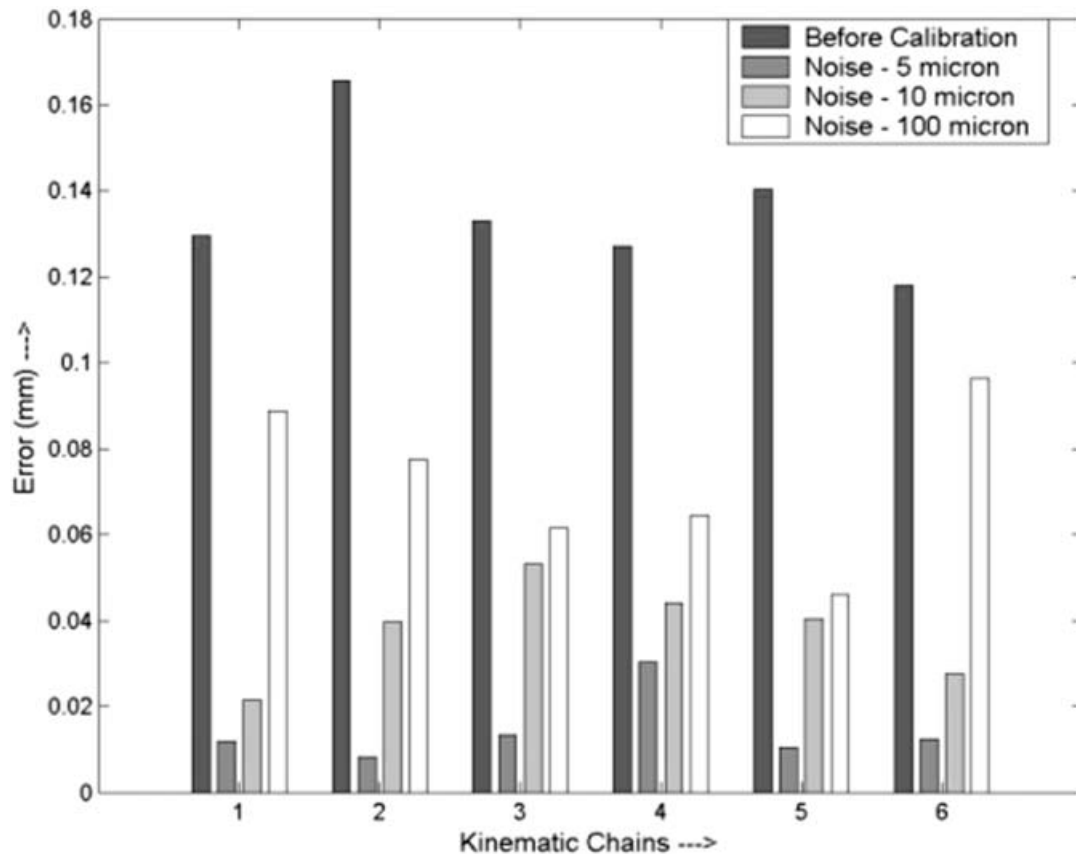


Fig. 7. Errors comparison for kinematic chains (with measurement noise).

rotations was chosen to be  $\pm 30^\circ$ . 30 postures were selected for calibration computations when the measurement noise was not considered, and 60 postures were used for the case of noisy measurements. Postures were selected from randomly generated valid set of postures by minimizing the condition number of the Identification Jacobian. Note that all parameters, except the angle between the measurement axes of the inclinometer, are linear. The condition number for the selected postures was around 900. QR analyses of the identification Jacobian showed that all of the parameters were identifiable.

Figure 6 shows the initial and the final errors for individual parameters for the third nominal set when measurement noise is not considered. In the figure, initial and final errors are represented, respectively, by the distance of '●' and '×' from the datum (0-line). Note that the final errors' marks appear on the datum line revealing that all parameters are identifiable. Identification with other nominal sets shows the same trend. Therefore, it can be concluded that identification is robust against the initial errors.

Uniformly distributed random noise was added to the exact measurements, including the articular variables, the rotary sensor measurements and the angles measured by inclinometers, to study noise effects. For angular measurements, a noise of 0.005 degree was added to the exact values. Note that this value of measurement noise is higher than the values considered in references [9] and [11]. For the articular variables, different levels of measurement noise were simulated. Figure 7 compares errors in the kinematic chains before and after calibration for different values of

Table III. Effects of measurement noise.

	Initial Error	Error after Calibration			
		5 $\mu$	10 $\mu$	50 $\mu$	100 $\mu$
Position	2.39 mm	27.45 $\mu$	53.6 $\mu$	157.8 $\mu$	241.4 $\mu$
Orientation	0.61°	0.013°	0.012°	0.044°	0.069°

measurement noise, and Table III compares the mean values of the errors in position and orientation for 50 randomly selected postures. Note that the height of bar in figure 7 represents norm of the errors for the corresponding kinematic chain. The nominal set 2 was used for the results shown below. Results show that even with high values of measurement noise, 100 micron, the improvement in accuracy is about 10 times.

## 5. CONCLUSIONS

A new measurement device is proposed for the calibration of parallel manipulators that can identify all kinematic parameters with partial pose measurements. The formulation for the calibration scheme, using the proposed device, is discussed for a six degree-of-freedom fully parallel Hexa Slide manipulator. The device, however, is general and can be used for other parallel manipulators. Computer simulations show that the calibration results are robust against errors in the initial guess and that errors can be significantly reduced by the proposed calibration device and procedure.

### Acknowledgement

This work was supported by the Korea Research Foundation Grant. (KRF-2003-041-D20039)

### References

1. J. M. Hollerbach and C. W. Wampler, "The calibration index and taxonomy for robot calibration methods," *Int. J. Robotic Research* **15**, No. 6, 573–591 (1996).
2. H. Zhuang, J. Yan and O. Masory, "Calibration of Stewart platforms and other parallel manipulators by minimizing inverse kinematic residuals," *Journal of Robotic Systems* **15**(7), 395–405 (1998).
3. A. Nahvi, J. M. Hollerbach and V. Hayward, "Calibration of parallel robot using multiple kinematic closed loops," *Proceedings of IEEE International Conference on Robotics and Automation* (1996) pp. 407–412.
4. P. Maurine and E. Dombre, "A calibration procedure for the parallel robot Delta 4," *Proceedings of IEEE International Conference on Robotics and Automation* (1996) pp. 975–980.
5. H. Ota, T. Shibukawa, T. Tooyama and M. Uchiyama, "Forward kinematic calibration method for parallel mechanism using pose data measured by a double ball bar system," *Proceedings of the Year 2000 Parallel Kinematic Machines International Conference* (2000) pp. 57–62.
6. Y. Takeda, G. Shen and H. Funabashi, "A DBB-based kinematic calibration method for inparallel actuated mechanisms using a fourier series," *Proceedings of DETC'02, ASME 2002 Design Engineering Technical Conferences and Computer and Information in Engineering Conference*, DETC2002/MECH-34345 (2002) pp. 1–10.
7. S. Besnard and W. Khalil, "Calibration of parallel robots using two inclinometers," *IEEE International Conference on Robotics and Automation* (1999) pp. 1758–1763.
8. H. Zhuang and L. Liu, "Self-Calibration of a class of Parallel Manipulators," *Proceedings of IEEE International Conference on Robotics and Automation* (1996) pp. 994–999.
9. H. Zhuang, "Self-calibration of parallel mechanisms with a case study on Stewart platforms," *IEEE Transactions on Robotics and Automation* **13**, No. 3, 387–397 (1997).
10. C. W. Wampler, J. M. Hollerbach and T. Arai, "An implicit loop method for kinematic calibration and its application to closed-chain mechanisms," *IEEE Transactions on Robotics and Automation* **11**, No. 5, 710–724 (1995).
11. W. Khalil and S. Besnard, "Self Calibration of Stewart-Gough parallel robots without extra sensors," *IEEE Transactions on Robotics and Automation* **15**, No. 6, 1116–1121 (1999).
12. P. Maurine, K. Abe and M. Uchiyama, "Towards more accurate parallel robots," *Proceedings of IMEKO-XV World Congress*, Osaka, Japan (1999) **Vol X**, pp. 73–80.
13. P. Maurine, M. Uchiyama and K. Abe, "A fully-autonomous procedure for kinematic calibration of HEXA parallel robots," *Proceedings of 1998 China-Japan Bilateral Symposium on Advanced Manufacturing Engineering*, Huangshan City, P. R. China (1998) pp. 161–166.
14. P. Maurine, D. M. Liu and M. Uchiyama, "Self-Calibration of a new HEXA parallel robot," *Proceedings of the 4th Japan-France Congress & 2nd Asia-Europe Congress on Mechatronics*, Kitakyushu, Japan (1998) pp. 290–295.
15. M. A. Meggiolaro, G. Scriffignano and S. Dubowsky, "Manipulator calibration using a single end-point contact constraint," *Proceedings of DETC2000: 2000 ASME Design Engineering Technical Conference*, DETC2000/MECH-14129 Baltimore, MD, (2000) pp. 1–8.
16. A. Rauf and J. Ryu, "Fully autonomous calibration of parallel manipulators by imposing position constrain," *Proceedings of IEEE International Conference on Robotics and Automation*, Seoul (2001) pp. 2389–2394.
17. J. Ryu and A. Rauf, "A new method for fully autonomous calibration of parallel manipulators using a constraint link," *Proceedings of AIM'01 conference*, Italy (2001) pp. 141–146.
18. I. Fassi and G. Legnani, "Automatic identification of a minimum, complete and parametrically continuous model for the geometrical calibration of parallel robots," *Proceedings of the Workshop on Fundamental Issues and Future Research Directions for Parallel Mechanisms and Manipulators*, Quebec, Canada (2002) pp. 204–213.
19. C. C. Iurascu and F. C. Park, "Geometric algorithm for parallel mechanism machine tool," *Proceedings of IEEE International Conference on Robotics and Automation* (1999) pp. 1752–1757.
20. D. Daney and I. Z. Emiris, "Robust parallel robot calibration with partial information," *Proceedings of IEEE International Conference on Robotics and Automation*, Seoul (2001) pp. 3262–3267.
21. W. Khalil, M. Gautier and Ch. Enguehard, "Identifiable parameters and optimum configurations for robots calibration," *Robotica* **9**, Part 1, 63–70 (1991).
22. M. P. Oliviers and J. R. Rene Mayer, "Global Kinematic Calibration of a Stewart Platform," *ASME Transactions on Dynamic Systems and Control Division* **57**(1), 129–136 (1995).
23. S. Besnard and W. Khalil, "Identifiable parameters for parallel robot kinematic calibration," *Proceedings of IEEE International Conference on Robotics and Automation*, Seoul (2001) pp. 2859–2866.
24. J. P. Merlet, *Les Robots Paralleles*, 2nd ed. (Hermes, Paris 1997).